Genomics 112 (2020) 3893–3902

Contents lists available at ScienceDirect

Genomics

journal homepage: www.elsevier.com/locate/ygeno

Population genetics and comparative mitogenomic analyses reveal cryptic diversity of *Amphioctopus neglectus* (Cephalopoda: Octopodidae)

Yan Tang[a,b], Xiaodong Zheng[a,b,*], Haijuan Liu[c], Feige Sunxie[d]

[a] Institute of Evolution and Marine Biodiversity, Ocean University of China, Qingdao 266003, China
[b] Key Laboratory of Mariculture, Ocean University of China, Qingdao 266003, China
[c] Guangxi Key Laboratory of Marine Biotechnology, Guangxi Institute of Oceanology, Beihai 536000, China
[d] Dongshan Boguangtianxing Foods Co., Ltd., Zhangzhou 363000, China

ARTICLE INFO

Keywords:
Amphioctopus neglectus
Cryptic diversity
cox1 and *cox3* genes
Genetic diversity
Mitogenome

ABSTRACT

This study presented 96 *cox1* and 76 *cox3* genes of *Amphioctopus neglectus* populations. Three distinct lineages were formed from phylogenetic trees and networks constructed using haplotypes. Mitogenomes of *A. neglectus*-a and *A. neglectus*-b as the representatives of two lineages separated from population genetics were sequenced to compare with *A. neglectus* at the genome-level. *Amphioctopus neglectus*-a showed significant differences with *A. neglectus*, mainly reflected in gene length, intergenic regions and the secondary structure of tandem repeat motifs. Notably, two sequence deletions in mitogenomes of the two representative species were detected in different positions of major non-coding regions, which were the most distinct differences with *A. neglectus*. Pairwise genetic distances and the phylogenetic analysis supported the relationship of (*A. neglectus*-a + (*A. neglectus* + *A. neglectus*-b)). This study suggested that *A. neglectus*-a should be considered as a potential cryptic species of this complex, while *A. neglectus*-b needed further verification to be defined.

1. Introduction

The Octopodidae is the largest family in the Octopoda (Mollusca: Cephalopoda). It is a taxon with high diversity, which can be found from the Arctic to the Antarctic, from the intertidal zone to depths greater than 3500 m [1–3]. It contains the vast majority of octopods, with more than 200 valid species [4]. By 2005, more than 150 undescribed species have been recognized through examination of museum collections, primary field surveys and discovery of many cryptic species [5]. Even so, there are still many uncertain species to be resolved, including many cryptic species [5]. Cryptic species are common among marine invertebrates [6], many of which lack identifiable delineating morphological traits [7]. In recent years, many molecular studies have made great contributions on taxonomy [4,5] and phylogeny [8–11], providing novel insight into cryptic species identification of Octopodidae [12,13]. A number of cryptic species were identified, as found for *Amphioctopus marginatus* in Taiwan [14]; Norman [15] has proposed that there were cryptic species for both *A. kagoshimensis* and *Hapalochlaena fasciata*; Xu et al. [13] indicated a divergent lineage among *Octopus minor* populations based on COI and 16S rRNA. In addition, the cryptic diversity of the *O. vulgaris* species complex has received great attention; several species in this complex are indistinguishable by morphological traits [5,16–19].

Data from mitochondrial genomes are well suited for phylogenetics, phylogeography, population genetics, and molecular ecology, owing to its maternal inheritance, lack of recombination and higher evolutionary rates [20–23]. Comparing mitogenomes among multiple related species can provide sufficient sequence data, which has been widely used and well described in metazoans [21]. For example, reports in insects, shellfish, reptiles, focused on the relationship between related species and subspecies according to the organization, arrangement and codon usage of genes in mitochondrial genomes [23–26]. Moreover, recent studies have shown that comparative analyses of mitogenomes were increasingly applied in species delimitation especially in cryptic species identification, providing evidence for the existence of cryptic species in some taxa (e.g. ascidian, shellfish, etc.) [27–30].

In this study, two mitochondrial genes, that is, cytochrome *c* oxidase subunit I (*cox1*) and III (*cox3*) were used in population genetic analysis. Typically, the *cox1* gene was the most conserved among cytochrome *c* oxidase subunits [31]. To date, the *cox1* gene has been regarded as a useful tool and widely used for coleoid species in efficiently identifying species, especially overlooked species [32–37]. Recently, the *cox3* gene was found to be useful for analyzing phylogeny among closely related shallow-water octopuses [9]. Considering the basis of population

* Corresponding author at: Institute of Evolution and Marine Biodiversity, Ocean University of China, Qingdao 266003, China.
E-mail address: xdzheng@ouc.edu.cn (X. Zheng).

https://doi.org/10.1016/j.ygeno.2020.06.036
Received 24 February 2020; Received in revised form 14 June 2020; Accepted 22 June 2020
Available online 27 June 2020

Table 1
Genetic diversity information of 7 populations of *A. neglectus* analyzed by *cox1* and *cox3* genes. Number of individuals of each population (N), number of polymorphic sites (V), number of haplotypes (Hap), haplotype diversity (Hd), nucleotide diversity (π), average number of nucleotide differences (k).

Sampling site	Abbr.	*cox1*						*cox3*					
		N	V	Hap	Hd	π	k	N	V	Hap	Hd	π	k
Dongshan	DS	11	4	4	0.600	0.00158	0.873	11	1	2	0.545	0.00120	0.545
Yangjiang	YJ	18	2	2	0.111	0.00040	0.222	18	4	4	0.314	0.00098	0.444
Beihai	BH	23	8	6	0.613	0.00179	0.988	8	7	3	0.464	0.00385	1.750
Sanya	SY	12	3	4	0.455	0.00091	0.500	12	4	4	0.561	0.00177	0.803
coastal waters of Pakistan	CWP	21	5	8	0.757	0.00185	1.019	15	4	3	0.562	0.00193	0.876
coastal waters of India	CWI-a	3	1	2	0.667	0.00121	0.667	5	2	3	0.700	0.00220	1.000
	CWI-b	8	2	3	0.464	0.00091	0.500	7	2	2	0.476	0.00210	0.952

genetic analysis in the present study, we sequenced the mitogenomes of two representatives of two lineages separated from *A. neglectus*. Both population genetics and comparative mitogenomic analyses will reveal cryptic biodiversity in *A. neglectus*. Moreover, phylogenetic analysis inferred in this study will be helpful to understand the evolutionary relationships within Octopodidae and determine the taxonomic status of the *A. neglectus* complex.

2. Materials and methods

2.1. Sample collection and DNA extraction

Populations of *A. neglectus* were sampled from the Northwest Pacific and North Indian Ocean. Our study using octopuses did not require ethical approval as they were collected from local artisanal fisheries. The samples are very common in local area, therefore, this study did not involve endangered or protected species. The sample regions included Dongshan (DS), Fujian; Yangjiang (YJ), Guangdong; Beihai (BH), Guangxi; Sanya (SY), Hainan; coastal waters of Pakistan (CWP) and India (CWI) (Table S1). One specimen sampled from the coastal waters of Vietnam (CWV) from GenBank was also included.

A small piece of mantle muscle tissue was obtained from each individual and preserved in 100% alcohol until total DNA was extracted by the CTAB method as modified by Winnepenninckx et al. [38]. All specimens were stored in 10% formalin for one week before being transferred to 95% alcohol, and then deposited as voucher specimens (voucher number: see Table S1) in Fisheries College, Ocean University of China.

2.2. PCR amplification and sequencing

The *cox1* and *cox3* fragments for population analysis were amplified through the use of primers LCO1490/HCO2198 [39] and Oco3F/Oco3R [9] in a volume of 50 μl, which contained 36.75 μl sterile distilled H_2O, 1 μl template DNA (approximately 100 ng), 5 μl 10 × buffer (Mg^{2+} plus), 5 μl dNTP (10 mM), 1 μl of each primers (10 μM), 0.25 μl (1 U) rTaq DNA polymerase. PCR was run under the following cycle condition: 94 °C for 3 min, followed by 36 cycles of denaturing at 94 °C for 45 s, annealing at 49 °C for 1 min, extending at 72 °C for 1 min, then extension at 72 °C for 10 min.

Two mitogenomes were concatenated using fragments with unequal length. Fourteen short mitochondrial fragments were amplified by polymerase chain reaction (PCR) with specific primers designed by Ma [40]. PCR amplifications were carried out in a 10 μl total volume containing 7 μl sterile distilled H_2O, 0.5 μl template DNA (approximately 100 ng), 1 μl 10 × buffer (Mg^{2+} plus), 1 μl dNTP (10 mM), 0.2 μl of each primer (10 μM), 0.1 μl (1 U) rTaq DNA polymerase. Given the costs of research and fidelity of polymerases [41,42], LA 10 × buffer (Mg^{2+} plus) and LA-Taq DNA polymerase were used for long PCR in above-mentioned 10 μl volume. Short mitochondrial fragments were amplified with the following cycling conditions: 94 °C for 3 min; 32 cycles of 94 °C for 45 s, 48 °C for 1 min, 72 °C for 1 min 20 s; and a final extension of 72 °C for 5 min. Long-PCR conditions included an initial denaturation step of 94 °C for 3 min, 35 cycles of 94 °C for 45 s, 42–60 °C for 1 min, 72 °C for 1 min 50 s, and a final extension step at 72 °C for 10 min. All PCR products were checked by 1.5% agarose gel electrophoresis, purified with EZ-10 Spin Column PCR Product Purification Kit (Sangon). Purified products were sequenced using an ABI 3730 automatic sequencer at Personalbio Biotechnology Company (Shanghai, China) via a primer-walking method. Several long-PCR fragments containing the non-coding region were cloned into the pEASY-T1 Cloning Vector (TransGen Biotech) and sequenced using M13 F/R universal primers.

2.3. Population genetic analysis

All contig sequences were assembled by SeqMan (DNASTAR software package). The modified sequences were aligned by Clustal W [43] using default settings in MEGA v.6.0 [44]. DnaSP v5.10 [45] was used to compute the number of haplotypes (Hap), the haplotype diversity (Hd), nucleotide diversity (π), number of variable sites (V) and average number of nucleotide differences (k) (Table 1). The haplotype networks were constructed using the median-joining method with default settings in Popart v.1.7 [46]. Two haplotype networks were visualized and manually adjusted. To guarantee reliability, Maximum Likelihood (ML) and Bayesian Inference (BI) approaches were used to verify the topology produced consistently. The ML analyses of the haplotypes were performed using RAxML37 web server on the CIPRES Science Gateway V.3.3 (http://www.phylo.org/index.php/) with 1000 replicates bootstrap values for node reliability estimation. The HKY + G and TIM3 models were selected as the best for *cox1* and *cox3* by jModelTest [47] based on the Akaike information criterion (AIC). The Bayesian inference (BI) analyses were conducted by MrBayes v.3.1 [48] using the HKY + G model for *cox1* and HKY model for *cox3*. The Markov chain Monte Carlo (MCMC) were run for 500,000 generations, with sampling every 100 generations and discarding the first 25% trees were as burnin. The standard deviation of split frequencies was less than 0.01. All parameters were checked using Tracer v 1.5 [49], and the effective sample size (ESS) for the log-likelihood was more than 200.

To evaluate hierarchical structure of variability, an analysis of molecular variance (AMOVA) was used to partition variance components attributable to population variance and to individuals within populations using Arlequin 3.5 [50]. We partitioned the eight populations into three groups based on lineage pattern, i.e., group 1 (CWI-a), group 2 (CWI-b) and group 3 (DS, YJ, BH, SY, CWV and CWP) (Table 2). Pairwise genetic divergence between populations was estimated with the fixation index (Fst) and assessed with exact tests based on 10,000 permutations.

2.4. Genome assembly, gene annotation and sequence analysis

Considering the basis of population genetic analysis, we sequenced

Table 2
AMOVA analysis for *A. neglectus* among different populations based on *cox1* and *cox3*.

Genes	Source of variation	df	Variance components	Percentage of variation
cox1	Among groups	2	6.48028	53.31*
	Among populations Within groups	5	5.30903	43.67*
	Within populations	89	0.36670	3.02
	Total	96	12.75468	
cox3	Among groups	2	11.98468	96.61*
	Among populations Within groups	5	0.01068	0.09
	Within populations	69	0.40970	3.30*
	Total	76	12.40505	

* Significant at $P < .05$.

complete mitochondrial genomes for two individuals collected in the coastal waters of India representing two lineages that we refer to as *A. neglectus*-a (OUC−201709090307) and *A. neglectus*-b (OUC−201709090313).

Protein coding genes (PCGs) were identified by ORF Finder (http://www.ncbi.nlm.nih.gov/orffinder) using the invertebrate mitochondrial code. Transfer RNA (tRNA) genes were determined using MITOS [51] and ARWEN [52]. The boundaries of rRNA genes were identified by comparing with the mitogenome of *A. neglectus* [25]. The tandem repeat sequences were searched by Tandem Repeats Finder 4.0 [53]. The secondary structures were predicted by the mfold version 3.2 web server [54] with default parameters. We chose the most stable (lowest free energy △G) one when there were more than one secondary structure. Codon usage of thirteen PCGs and nucleotide of mitogenomes were estimated by MEGA v.6.0 [44]. AT and GC skews for a given strand was calculated as: AT skew = (A − T) / (A + T), GC skew = (G − C) / (G + C) [55]. Gene maps of two mitogenomes were calculated with the program CGView [56]. The ratios of nonsynonymous and synonymous substitution rates (Ka/Ks) were estimated using Ka_Ks calculator 2.0 [57] with the NG model. The pairwise genetic distance for PCGs were estimated using MEGA v6.0 [44] based on the Kimura-2-−arameter (K2P) model with 1000 bootstraps.

2.5. Phylogenetic analysis

A total of 16 mitochondrial genome sequences were selected for phylogenetic analysis (Table S2). *Vampyroteuthis infernalis* (NC009689) from family Vampyroteuthidae and *Argonauta hians* (KY649285) from family Argonautidae were used as outgroups. The 13 PCGs were also aligned using by Clustal W [43] in MEGA v.6.0 [44]. The concatenation of genes was performed using SequenceMatrix v1.7.8 [58] spanning 11,124 nucleotide positions. We performed the phylogenetic analyses by ML and BI method. ModelFinder [59] plugin integrated into IQ-TREE v1.6.12 [60] was used to calculate the best-fit partitioning scheme automatically. The best partition scheme and substitution models were listed in Table S3. Then ML analyses were carried out using IQ-TREE v1.6.12 [60] under Edge-linked partition model for 1000 bootstraps replicates. PartitionFinder v2.1.1 [61] based on the Akaike Information Criterion (AIC) was used to estimate the optimal partition strategy and best-fit evolution model of each partition for BI analysis (Table S3). BI analyses were performed by MrBayes v3.2.6 [48] with the linked branch lengths of each partition scheme with 2,000,000 generations under the Markov chain Monte Carlo (MCMC) command, sampling every 100 generations. The first 25% generations were discarded as burn-in, and a consensus tree (BI tree) was generated. Convergence of the parameters in use was checked with Tracer v1.5 [49], and the ESS value was more than 200. All phylogenetic results were visualized using FigTree v1.4.3 (http://tree.bio.ed.ac.uk/software/figtree).

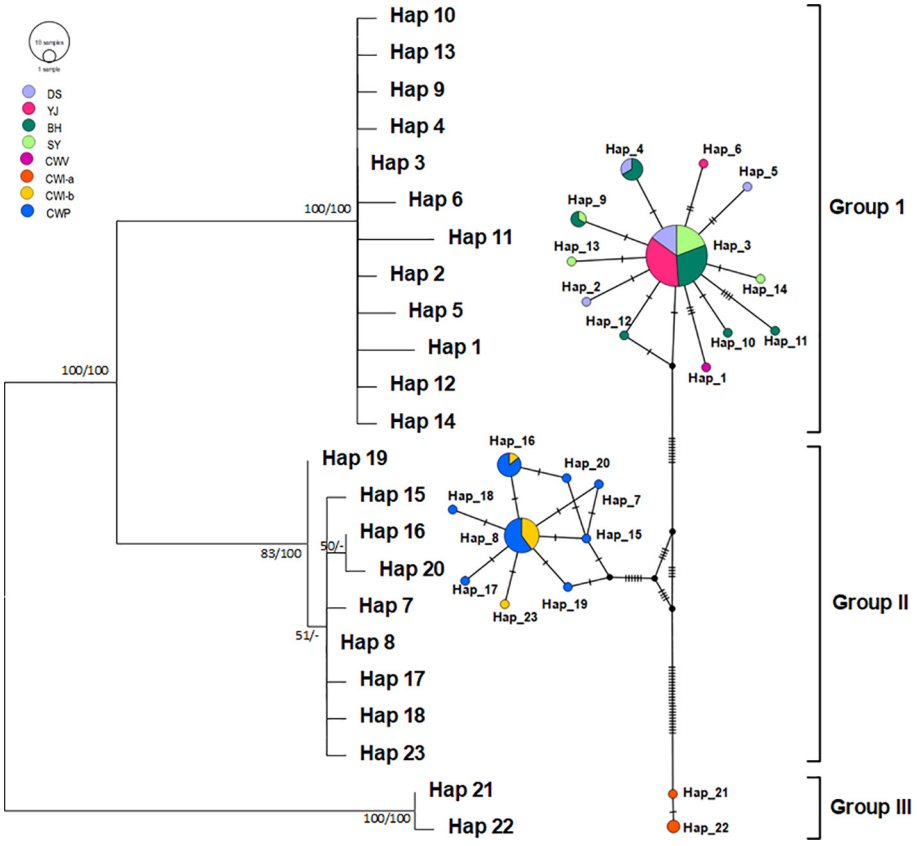

Fig. 1. Maximum likelihood (ML) and Bayesian inference (BI) phylogenetic tree and haplotype network of *A. neglectus* based on *cox1* haplotypes. Branch numbers are bootstraps (left) and posterior probability (right). Size of circle is proportional to the frequency of a particular haplotype. Each small line on the line that connects two circles represents a mutational step and black dots represent hypothetical missing intermediates.

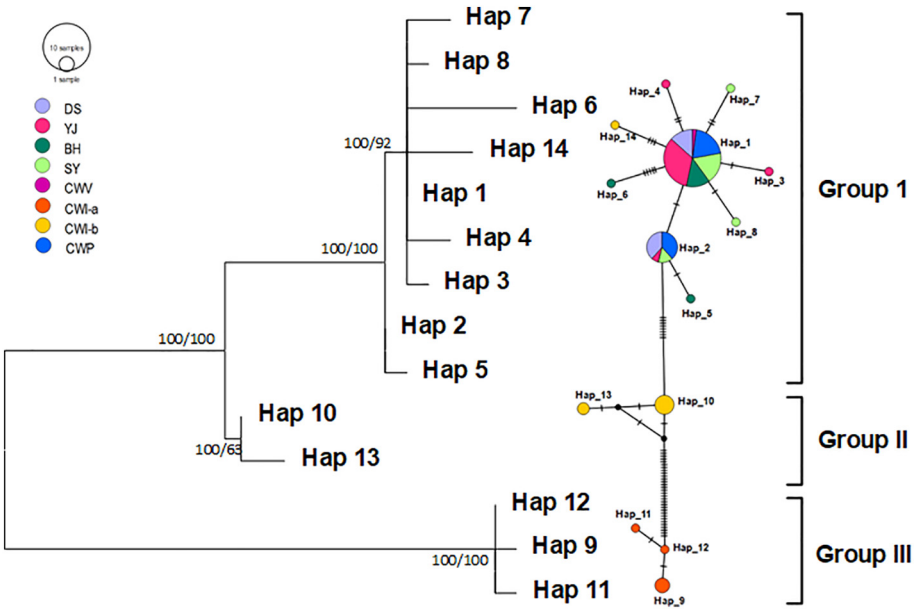

Fig. 2. Maximum likelihood (ML) and Bayesian inference (BI) phylogenetic tree and haplotype network of *A. neglectus* based on *cox3* haplotypes. Branch numbers are bootstraps (left) and posterior probability (right). Size of circle is proportional to the frequency of a particular haplotype. Each small line on the line that connects two circles represents a mutational step and black dots represent hypothetical missing intermediates.

3. Results

3.1. Population genetic analysis

The ML tree and haplotype network based on 23 *cox1* haplotypes observed show a consistent topology, which shows three distinct groups (Fig. 1). Haplotypes (Hap) 21 and 22 from the coastal waters of India (CWI) clustered together and diverged early. Subsequently, other CWI haplotypes and all CWP haplotypes were assigned into one cluster with strong nodal support. Here, we designated these two groups of CWI as CWI-b and CWI-a, respectively. Other haplotypes consist of individuals from the coastal waters of China (DS, YJ, BH, SY) and Vietnam (CWV) clustered into Group I (Fig. 1). In the *cox1* network, Hap 3 was the most prevalent haplotype shared by 47 individuals from 4 populations. Notably, Group II and III were clearly separated by many more mutational steps with Group I, successively. The *cox3* ML tree and network differed from those based on *cox1* in that all CWP haplotypes were gathered into Group I, and shared the Hap 1, 2 with haplotypes from the coastal waters of China (DS, YJ, BH, SY). Hap 9, 11, 12 which are exclusive for CWI-a samples were separated by more than 30 mutational steps from CWI-b haplotypes (Fig. 2).

Furthermore, we identified 25 polymorphic sites and 29 haplotypes in the 96 partial *cox1* sequences (551 bp). The highest (Hd = 0.757) and lowest (Hd = 0.111) haplotype diversity was defined in the CWP and YJ population, respectively (Table 1). Similarly, the nucleotide diversity (π) and average number of nucleotide differences (k) were the highest in CWP, and the lowest in YJ (Table 1). The partial *cox3* (454 bp) sequences showed a slightly different pattern (Table 1). Twenty-four polymorphic sites and 21 haplotypes were found in 76 specimens. Nucleotide diversity (π) and average number of nucleotide differences (k) showed similar results that two indices are much lower in YJ than those in the CWP population (Table 1). CWI-a had a high haplotype diversity, and YJ had a relatively low haplotype diversity, of which the populations ranged from 0.314 to 0.700.

The AMOVA analysis based on *cox3* showed that the most of variance components were detected among groups (11.98468). The significant variation among groups (96.61%) could be explained by genetic variation between the inferred lineages, supporting the observation that the CWI-a population, CWI-b population and the remaining six populations have developed into three distinct lineages. In contrast, the analysis based on *cox1* showed higher variation (43.67%) among populations within groups, which might be explained that CWP population belong to two different groups in phylogenetic analysis constructed using *cox1* and *cox3* (Table 2).

3.2. Genome structure, organization and composition

In this study, we chose to call CWI-a "*A. neglectus*-a" and CWI-b "*A. neglectus*-b". To investigate the relations among this complex, a complete mitogenome sequence for *A. neglectus* (MH899749) from GenBank was also included (Table 3). Two mitogenomes were completely sequenced, characterized and submitted to GenBank with accession numbers MT080810 and MT080811 (Tables S2). The sequences were found to be 15,747 bp for *A. neglectus*-a and 15,668 bp for *A. neglectus*-b in size, which were a little shorter than that for *A. neglectus* (Fig. S1, Table 3). Each mitogenome comprised 13 protein-coding genes (PCGs), 22 tRNAs, 2 rRNAs (*rrnS* and *rrnL*), and a major non-coding region (MNR) between the *trnP* and *cox3* genes. Fifteen of the 37 genes were encoded by the plus strand, with the others encoded by the minus strand (Fig. S1, Table 3).

The nucleotide compositions and AT contents of three mitogenomes were similar with each other (Table S4). The AT contents of the three mitogenomes ranged from 75.09% to 75.76%. The three mitogenomes all showed positive AT skews and negative GC skews, which indicated skew away from T in favor of A, and G in favor of C (Table S4).

3.3. Protein-coding genes, tRNA and rRNA genes

All PCGs used ATR and TAR as initiation and termination codons consistently in three species (Table 3). Eight of thirteen PCGs started with ATG, and ten of thirteen PCGs terminated with TAA. All PCGs shared the same gene length except for *nad2* and *nad4* of *A. neglectus*-a, which were longer than those of *A. neglectus* and *A. neglectus*-b. High AT contents were detected in all PCGs, and the maximum negative and positive AT skews of three species were identical in *cytb* and *cox2*, respectively. The maximum positive GC skews were all detected in *nad6*, while the maximum negative GC skews of *A. neglectus*-a differed from the others (Table S4). The 22 typical tRNAs were interspersed between PCGs and rRNAs. The tRNAs were similar to each other and ranged from 64 bp to 71 bp in size. Two rRNA genes were separated by a *trnV* gene. The lengths of *rrnL* in the three species were 1314 bp, 1315 bp and 1321 bp, and the lengths of *rrnS* were 960, 964 and 968 bp, respectively.

Thirteen, twelve and fourteen overlaps between adjacent genes

Table 3
Organization of the mitogenome of *Amphioctopus neglectus* (AN), *A. neglectus*-a (ANa) and *A. neglectus*-b (ANb).

Gene	Size (bp)			Start codons			Stop codon			Strand	Intergenic regions		
	AN	ANa	ANb	AN	ANa	ANb	AN	ANa	ANb		AN	ANa	ANb
cox3	780	780	780	ATG	ATG	ATG	TAA	TAA	TAA	+	663	582	502
trnK(*ttt*)	69	67	69							+	8	8	8
trnA(*tgc*)	68	68	70							+	−2	−2	−2
trnR(*tcg*)	64	65	64							+	0	0	−1
trnN(*gtt*)	67	67	67							+	0	0	0
trnI(*gat*)	67	67	67							+	0	0	0
nad3	357	357	357	ATA	ATA	ATA	TAA	TAA	TAA	+	−6	−6	−6
trnS1(*gct*)	69	69	69							+	−2	−2	−2
nad2	1056	1182	1056	ATA	ATA	ATA	TAA	TAA	TAA	+	−18	−18	−18
cox1	1533	1533	1533	ATG	ATG	ATG	TAA	TAA	TAA	+	−29	−155	−29
cox2	687	687	687	ATG	ATG	ATG	TAA	TAA	TAA	+	6	6	6
trnD(*gtc*)	67	67	67							+	−2	−2	−2
atp8	156	156	156	ATG	ATG	ATG	TAA	TAA	TAA	+	1	1	1
atp6	693	693	693	ATG	ATG	ATG	TAG	TAG	TAG	+	1	1	1
trnF(*gaa*)	67	68	67							−	24	25	24
nad5	1737	1737	1737	ATG	ATG	ATG	TAA	TAA	TAA	−	−44	−44	−44
trnH(*gtg*)	65	64	65							−	0	0	0
nad4	1344	1338	1344	ATA	ATA	ATA	TAA	TAA	TAA	−	3	3	3
nad4l	306	306	306	ATA	ATA	ATA	TAG	TAG	TAG	−	−4	2	−4
trnT(*tgt*)	64	64	64							+	−5	−5	−5
trnS2(*tga*)	66	66	66							−	2	2	2
cytb	1146	1146	1146	ATA	ATA	ATA	TAA	TAA	TAA	−	−2	−2	−2
nad6	513	513	513	ATG	ATG	ATG	TAG	TAG	TAG	−	−14	−14	−14
nad1	942	942	942	ATG	ATG	ATG	TAA	TAA	TAA	−	74	74	74
trnL2(*taa*)	71	71	71							−	0	0	0
trnL1(*tag*)	65	65	65							−	0	0	0
rrnL	1314	1315	1321							−	3	3	3
trnV(*tac*)	69	69	69							−	−3	−3	−3
rrnS	960	964	968							−	4	6	6
trnM(*cat*)	68	68	68							−	−1	−1	−1
trnC(*gca*)	65	65	65							−	3	3	3
trnY(*gta*)	64	64	64							−	0	0	0
trnW(*tca*)	66	67	66							−	0	0	0
trnQ(*ttg*)	68	68	68							−	0	0	0
trnG(*tcc*)	66	66	66							−	3	3	3
trnE(*ttc*)	71	71	71							−	5	6	5
trnP(*tgg*)	70	70	70							−	146	152	143

were found in the three mitogenomes, ranging from 1 bp to 155 bp in length. A 1 bp overlap between *trnA* and *trnR* was detected in *A. neglectus*-b, which was absent in *A. neglectus* and *A. neglectus*-a. Between *nad4* and *nad4l*, 4 bp overlaps were detected in all species except for *A. neglectus*-a. In the mitogenome of *A. neglectus*-a, there is a 155 bp overlap between *nad2* and *cox1*, which differs from the other two mitogenomes (Fig. 4).

3.4. Non-coding intergenic region

Fifteen to sixteen non-coding intergenic regions were interspersed throughout the three mitogenomes (Fig. 4, Table 3). *Amphioctopus neglectus*-b was congruent with *A. neglectus* in number of intergenic regions, while a 2 bp intergenic region was detected between *nad4* and *nad4l* in the *A. neglectus*-a mitogenome. Four non-coding intergenic regions could be found larger than 10 bp: 1) *atp6-trnK*; 2) *nad6-nad1*; 3) *trnE-trnP* and 4) *trnP-cox3*. The intergenic region located between *trnP* and *cox3* is the largest, which was defined as major non-coding region (MNR), with the variation among the three specimens in length (Fig. 4). AT contents of this regions were much higher than GC contents in the three mitogenomes. AT skew of *A. neglectus*-a is much lower than those of the others, which indicated skews of the latter are far away from T in favor of A (Table S4). Compared with *A. neglectus*, the MNRs of *A. neglectus*-a and *A. neglectus*-b were truncated in different positions (Figs. 4, 5). In each MNR, a conserved sequence block was detected located between two nonconservative regions. Several distinct tandem repeat motifs (TRMs) could be detected in the three MNRs and folded into stem-loop secondary structures under minimized free energy (Fig. 5). Four TRMs (1, 3, 4, 5) were detected in *A. neglectus* (Fig. 5A). The former three TRMs were specific for *A. neglectus*, of which the TRM3 and TRM4 were found in the conserved region, with several bases difference from *A. neglectus*-a and *A. neglectus*-b (Fig. 5A). TRM5 in *A. neglectus* and TRM6 in *A. neglectus*-b were consistent and were predicted to be the same stem-loop structures (Fig. 5). TRM2 found in *A. neglectus*-a was composed of two stem-loop structures with high AT contents (Fig. 5B).

3.5. Nonsynonymous and synonymous substitution

In order to detect the influence of selection pressure in *Amphioctopus* mitogenomes, the pairwise ratios of non-synonymous (Ka) and synonymous (Ks) substitution of 13 PCGs were calculated among eight *Amphioctopus* species (Fig. 3). The values varied from 0 (between *A. neglectus* and *A. neglectus*-b in *cox1*, *cytb*, *nad6*) to 0.773 (between *A. neglectus* and *A. fangsiao* in *nad4l*). Overall, the Ka/Ks values in *nad4l*, *nad6*, *atp8* were higher than those in *cox1*, *cox2*, *cytb*.

3.6. Interspecific genetic distance and phylogenetic analysis

Pairwise genetic distances based on 13 PCGs within the *A. neglectus* complex ranged from 0.027 to 0.065, which was lower than those within other octopods (0.077–0.238). Genetic distance between *A. neglectus*-a and *A. neglectus*-b (0.027) was lower than any other pairwise genetic distances, while the distance between *A. neglectus*-a and *A. neglectus* (0.065) was close to that between *A. rex* and other species of the *A. neglectus* complex (0.077–0.079) (Table 4).

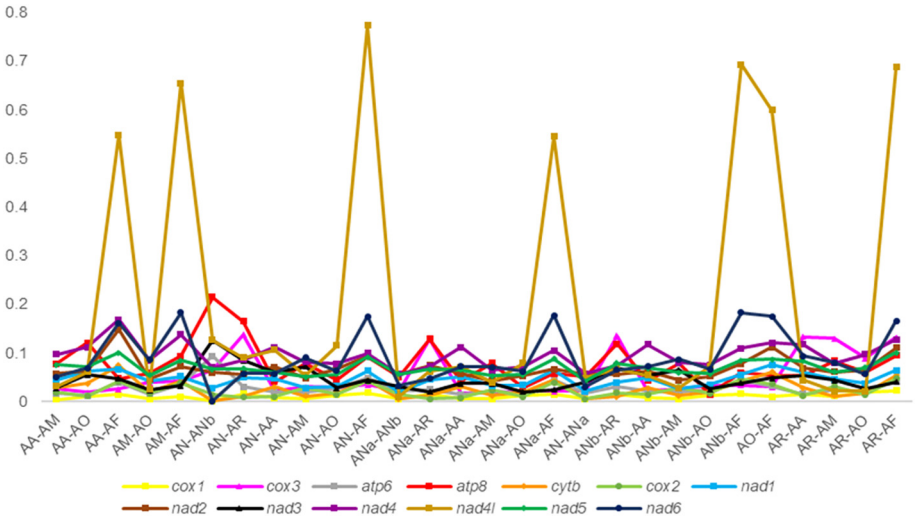

Fig. 3. The ratio of nonsynonymous and synonymous substitutions (Ka/Ks) estimated in all 13 protein genes of eight species of *Amphioctopus*. AA, *Amphioctopus aegina*; AF, *A. fangsiao*; AM, *A. marginatus*; AN, *A. neglectus*; ANa, *A. neglectus*-a; ANb, *A. neglectus*-b; AO, *A.* cf. *ovulum*; AR, *A. rex*.

Both construction methods of ML and BI revealed phylogenetic trees of identical topology (Fig. 6). *Argonauta hians* was sister to the rest of the octopuses within Octopoda in phylogenetic tree. In Octopodidae, the phylogenetic tree supported a polyphyletic genus of the *Octopus* and two monophyletic genera (*Amphioctopus* and *Cistopus*) with high support values. *Octopus conispadiceus* and *O. minor* were recovered at the deeper nodes. The other members of *Octopus* clustered into one group, and this group was sister to *Cistopus*. In the genus *Amphioctopus*, the relationship of (*A. neglectus*-a + (*A. neglectus* + *A. neglectus*-b)) was supported strongly.

4. Discussion

4.1. Population genetic analysis

Both phylogenetic trees and haplotype networks showed three distinct groups of *A. neglectus*, which were separated by many mutational steps and are likely to represent at least two separate lineages of *A. neglectus* in India. In *cox1* analysis, Group I contained specimens from coastal waters of China and Vietnam. Group II was formed by specimens from Pakistan and India, which differed from that in the *cox3* analysis. The different topologies were supposed to be associated with the different conserved gene sequences within *A. neglectus* complex. In most metazoans, three subunits of the cytochrome *c* oxidase and cytochrome *b* had a higher degree of conservation than NADH dehydrogenase genes [62]. In any case, all haplotypes in CWI gathered into Group II and III in both *cox1* (Fig. 1) and *cox3* (Fig. 2) analysis, indicating that at least two highly divergent mitochondrial cryptic lineages exist in *A. neglectus* populations.

In this study, the CWI and CWP populations differed from the other *A. neglectus* populations, which may be due to the ocean currents. Ocean currents are an important factor in the genetic exchange of marine organisms and play a key role in population structure of cephalopods [63–65]. In contrast to the other populations, CWI and CWP are located in the northern Indian Ocean, where the influence of the southern subtropical monsoon climate creates a peculiar northern Indian Ocean monsoon circulation. The formation of the CWI-a population may be related to the ocean eddy located in Bay of Bengal in the Indian Ocean, which may reduce gene flow between the inside- and outside-of eddy populations. Due to the monsoonal currents, genetic exchange between other Indian population located outside the eddy (i.e. CWI-b) and the CWP population may occur, which may account for the clustering of CWP and CWI-b populations in the *cox1*-based haplotype network analysis.

The π value is important in terms of population genetic variations [13,66]. The relatively high genetic diversity of BH population might be attributed to large population sizes within their natural habitats [67]. Overall, the π value of *cox3* is higher than that of *cox1*, which may

Table 4
Interspecies genetic distance of *A. neglectus* (AN), *A. neglectus*-a (ANa), *A. neglectus*-b (ANb), *A. rex* (AR), *A. marginatus* (AM), *A. aegina* (AA), *A.* cf. *ovulum* (AcO), *A. fangsiao* (AF), *Cistopus chinensis* (CC), *C. taiwanicus* (CT), *Octopus bimaculatus* (OB), *O. vulgaris* (OV), *O. minor* (OM) and *O. conispadiceus* (OC) under K2P model based on 13PCGs.

	AN	ANa	ANb	AR	AM	AA	AcO	AF	CC	CT	OB	OV	OM	OC
AN	–													
ANa	0.065													
ANb	0.027	0.061												
AR	0.079	0.079	0.077											
AM	0.104	0.103	0.101	0.103										
AA	0.125	0.126	0.122	0.118	0.124									
AcO	0.118	0.122	0.118	0.117	0.123	0.122								
AF	0.149	0.155	0.152	0.146	0.152	0.146	0.147							
CC	0.199	0.206	0.199	0.189	0.198	0.190	0.196	0.180						
CT	0.193	0.201	0.192	0.188	0.197	0.188	0.190	0.177	0.133					
OB	0.182	0.191	0.181	0.185	0.188	0.178	0.185	0.171	0.179	0.174				
OV	0.187	0.192	0.187	0.188	0.188	0.186	0.191	0.178	0.184	0.181	0.145			
OM	0.226	0.228	0.226	0.219	0.224	0.216	0.218	0.207	0.212	0.212	0.204	0.207		
OC	0.233	0.238	0.232	0.229	0.234	0.230	0.228	0.220	0.226	0.226	0.225	0.231	0.222	–

account for the differences in phylogeny and haplotype network based on *cox1* and *cox3* analyses.

The genetic divergence of the *A. neglectus* complex was best explained by the variation between lineages, with the AMOVA suggesting that differences between CWI and remaining populations explained most of the genetic variance within *A. neglectus* complex, consistent with the phylogenetic analyses and the haplotype networks (Fig. 1-2). Both AMOVA analyses supported that CWI-a and CWI-b could be two lineages due to their genetic heterogeneity.

4.2. General features of three mitogenomes

Compared with the mitogenome of *A. neglectus* reported before [25], two newly sequenced mitogenomes in this study shared similar features. The three species share the same genome arrangement with a translocation of *trnP*, which differed from the typical pattern reported before [40,68–73]. Moreover, three mitogenomes showed typical patterns of skews (positive AT skews vs. negative GC skews), which were detected as a common feature of Cephalopods [74]. The strand asymmetry was explained by the frequent deamidation of the adenine and cytosine in single-stranded DNA, and the specific pairing [74,75]. To be specific, when DNA exposed as single-stranded, deamination of A nucleotide yields hypoxanthine, pairing with C rather than T, while deamination of C nucleotide yields uracil, pairing with A instead of G, leading to an excess of A relative to T and an excess of C relative to G.

Overlaps between adjacent genes are widely distributed and varied in many mitogenomes in animals [76,77]. The three mitogenomes are highly compact, which is common in octopods with over 90% of the genome encoding for structural genes [71]. Thus, many overlaps were recognized between adjacent genes in the present study, most of which are consistent in size. The differences of overlaps among three mitogenomes are reflected in the addition (*trnA-trnR* in *A. neglectus*-b), deletion (*nad4-nad4l* in *A. neglectus*-a) and variation in length (*nad2-cox1* in *A. neglectus*-a) due to the varied sizes of adjacent genes. The unique overlap between *nad2* and *cox1* in *A. neglectus*-a was also reported in *Cistopus chinensis* with the same position and length [71].

The non-coding intergenic regions among three mitogenomes are similar both in size and in number (Fig. 4), of which the variation reflected a positive correlation between mitogenome size and the length of non-coding regions [78]. Each mitogenome contains one MNR, which has been frequently observed in other cephalopods [79]. The highly conserved part of the MNR was colored in Fig. 5A and was detected with poly-T stretches, TRMs and high AT contents, which is typically believed to play an important role in sequence transcription initiation and replication in animal mitochondrial DNA [80–83]. Tandem repeat motifs were predicted to be stem-loop structures and varied within three MNRs except for the TRM5 in *A. neglectus* and TRM6 in *A. neglectus*-b (Fig. 5). In addition, the sequence deletions of MNRs were detected in *A. neglectus*-a and *A. neglectus*-b, which can be explained by slippage events that occur in regions with high AT contents [84]. Without regard to the regions with sequence deletions, a non-conservative region was detected (Fig. 5A), showing another main difference within three MNRs.

4.3. Nonsynonymous and synonymous substitution

The Ka/Ks is a crucial value in exploring the evolutionary dynamics of PCGs across closely related species [30,85,86]. Selective pressure in PCGs has been widely studied in marine invertebrates, revealing a pattern of widespread purifying selection [30,86,87]. In the present study, the Ka/Ks ratios were less than 1, indicating the existence of purifying selection among all species. The PCGs of *cox1*, *cox2*, *cytb* have much lower Ka/Ks rates compared with those of *nad4l*, *nad6*, *atp8*, indicating that the former are evolving under stronger purifying selection and evolutionary constraints [88]. Notably, *nad4l* showed an exceptionally high Ka/Ks ratio by comparison with the other protein-coding genes, suggesting it still have potential for positive selection in *nad4l* gene [86]. The Ka/Ks ratio close to 1 was also observed in *nad2* gene of other invertebrate (e.g. clams) and vertebrate mitochondrial genomes (e.g. fishes). As a PCG immediately upstream of the MNR in above mitogenomes, the *nad2* genes were exposed as single-stranded for the longest time during replication, rendering it more likely to accumulate mutations in the highly mutagenic environment of the mitochondrion [86,89]. In our study, the *nad4l* were located in the middle of 13 PCGs, suggesting a large distance from the origin of replication. Thus, the reason why the *nad4l* showed an exceptionally high Ka/Ks ratio merited further study. Additionally, the Ka/Ks ratio of *cox3* was higher than that of *cox1*, which may reflect lower purifying selection in the former than in the latter, and supporting the general observation that *cox1* shows a higher degree of conservation than *cox3*.

4.4. Interspecific genetic distance and phylogenetic analysis

In this study, the pairwise genetic distances were obtained based on 13 PCGs within 14 octopods, involving *Amphioctopus*, *Cistopus* and *Octopus*. Without regard to the extreme values produced by *A. neglectus*-a, the overall mean genetic distance of the genus *Amphioctopus* (0.120) is lower than those in *Cistopus* (0.133) and *Octopus* (0.206). This could be explained by the fact that *Octopus* radiated earlier than *Cistopus* and *Amphioctopus*. On the other hand, this phenomenon also indicated the closer relationships within the members of *Amphioctopus*. The genetic distance between *A. neglectus*-a and *A. neglectus* is quite similar to the lowest pairwise distances within congeneric species in *Amphioctopus*, which indicated that *A. neglectus*-a might be a cryptic species of *A. neglectus* complex.

In the Octopodidae, the phylogenetic analyses showed that the deeper nodes of the tree were reconstructed as *O. conispadiceus* and *O. minor*. Other two *Octopus* species grouped together and clustered into a sister taxon with the genus *Cistopus*. The polyphyly of the genus *Octopus* was clearly supported, which has been found in many studies [9,90,91]. *Amphioctopus neglectus* and *A. neglectus*-b were sister taxa and have a close relationship with *A. neglectus*-a, *A. rex*, *A. marginatus*, *A. aegina*, *A.* cf. *ovulum* and *A. fangsiao*, successively, which was consistent with the long-established theory that the genus *Amphioctopus* is monophyletic [25,40,72]. This phylogenetic analysis provided further evidence that the variation of overall mean genetic distance above could be due to differences in divergence times among genera. Moreover, the phylogenetic trees constructed based on the concatenation of 13 PCGs and haplotypes of two genes showed congruent topologies of (*A. neglectus*-

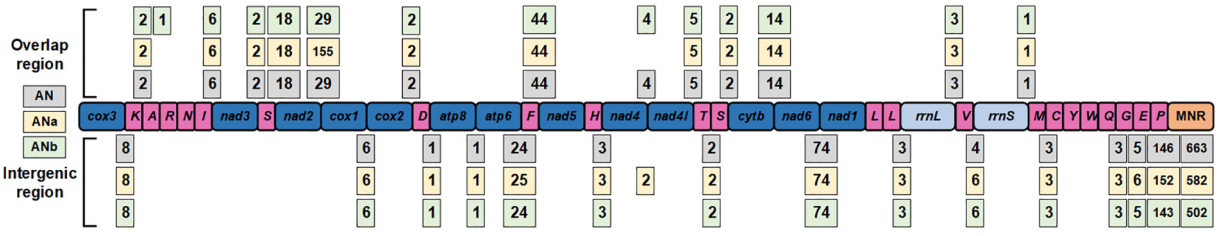

Fig. 4. Intergenic regions (below the gene ruler) and overlaps (above the gene ruler) in *A. neglectus* (AN), *A. neglectus*-a (ANa) and *A. neglectus*-b (ANb) mitogenomes.

Fig. 5. Major non-coding region. (A) Sequences of *A. neglectus* (AN), *A. neglectus*-a (ANa) and *A. neglectus*-b (ANb). (B) Stem-loop structures of the tandem repeat motifs.

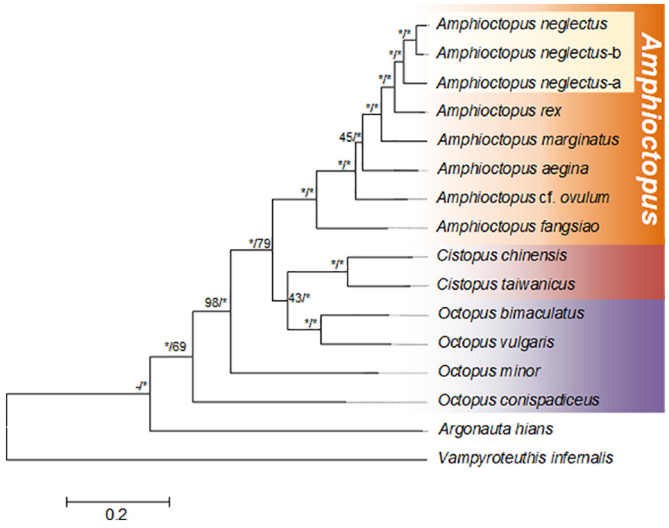

Fig. 6. Phylogenetic trees derived from maximum likelihood (ML) and Bayesian inference (BI) analyses based on the concatenation of 13 protein-coding genes. The first number at each node is the bootstrap of ML tree and the second number is posterior probability of BI tree. Each value of 100% is represented by an asterisk.

a + (*A. neglectus* + *A. neglectus*-b)), shedding light on the possibility of the cryptic species of this complex. Interestingly, these species are of extremely high external morphological similarity. Because the specimens are damaged during collection, we measured only a portion of available characters. Our unpublished morphometric data indicated that all these characters (i.e., mantle length, mantle width, head width, arm length, hectocotylus suckers count, ocellus ring width) are shared by *A. neglectus*-a and *A. neglectus*-b. We were unable to find any morphological difference among the complex. Cryptic species with no morphological differences but distinct genetic differences (cryptic species) have frequently been found in previous studies. Khatami et al. [92] identified potential cryptic species of *Sepia*, *Amphioctopus* and *Uroteuthis*, but found no morphological difference among the genetically distinct groups they proposed as cryptic species. Carlini et al. [93] demonstrated the existence of three distinct clades of North Atlantic *Illex* species with undistinguishable morphological characters. Moreover, this situation was also reported for other marine organisms [94–96]. Typically, boundaries between species become increasingly evident with the progress of the speciation process. De Queiroz [97] has proposed a point known as the grey zone that the boundaries between the species may be difficult to identify due to incipient speciation process. This might be the reason for the undistinguishable morphological characters among species with distinct genetic differences.

5. Conclusion

In the present study, we explored population genetic diversity of *A. neglectus* by comparing the number of polymorphic sites, number of haplotypes, haplotype diversity, nucleotide diversity, average number of nucleotide differences, and constructing phylogenetic tree and haplotype network using *cox1* genes of 96 samples and *cox3* genes of 76 samples, respectively. In addition, we determined two mitogenomes of the representative species separated in the population genetic analyses above. Phylogenetic analysis in the context of available mitogenome data of 16 octopods was also performed. The main findings are as follows: a) the cryptic diversity of *A. neglectus* is inferred according to the phylogeny and network based on population haplotypes; b) *Amphioctopus neglectus*-a differs from *A. neglectus* in gene length, intergenic regions and the secondary structure of tandem repeat motifs in MNR; c) *Amphioctopus neglectus*-b shows a little difference within three species mainly reflected in the non-coding region; d) the topology of (*A. neglectus*-a + (*A. neglectus* + *A. neglectus*-b)) is strongly supported in present phylogenetic analysis.

In a word, this study shed light on the presence of the cryptic diversity of *A. neglectus* complex. Our population genetics and comparative mitogenomic analyses presented the possibility of cryptic species, that is, *A. neglectus*-a. Nevertheless, a further verification is still needed to clarify whether *A. neglectus*-b can be defined as species or subspecies level.

Supplementary data to this article can be found online at https://doi.org/10.1016/j.ygeno.2020.06.036.

Declaration of Competing Interest

The authors declare that they have no competing financial interests.

Acknowledgments

This work was supported by the National Natural Science Foundation of China under Grant 31672257; Fundamental Research Funds for the Central Universities under Grant 201822022.

References

[1] J.R. Voight, A cladistic reassessment of octopodid classification, Malacologia 35 (1993) 343–349.
[2] K.L. Lamprell, J.M. Healy, A.M. Scheltema, K. Gowlett-Holmes, C.C. Lu, Zoological Catalogue of Australia Volume 17.2: Mollusca: Aplacophora, Polyplacophora, Scaphopoda, Cephalopoda (Zoological Catalogue of Australia Series), CSIRO Publishing, Melbourne, 2001.
[3] M. Nixon, J.Z. Young, R.E. Allen, J.Z. Young, The Brains and Lives of Cephalopods, Oxford University Press, 2003.
[4] M.D. Norman, J.K. Finn, F.G. Hochberg, Family Octopodidae, in: P. Jereb, C.F.E. Roper, M.D. Norman, J.K. Finn (Eds.), Cephalopods of the World. An Annotated and Illustrated Catalogue of Cephalopod Species Know to Date: Octopods and Vampire Squids, FAO, FAO species catalogue for fishery purposes. Rome, Italy, 2013, pp. 75–76.
[5] M.D. Norman, F.G. Hochberg, The current state of octopus taxonomy. Proceedings of the international workshop and symposium of cephalopod international advisory council, Phuket, Phuket Marine Biological Center Research Bulletin 66 (2005) (2003) 127–154.
[6] N. Knowlton, Sibling species in the sea, Annu. Rev. Ecol. Evol. S. 24 (1993) 189–216.
[7] M. Klautau, C.A. Russo, C. Lazoski, N. Boury-Esnault, J.P. Thorpe, A.M. Solé-Cava, Does cosmopolitanism result from overconservative systematics? A case study using the marine sponge *Chondrilla nucula*, Evolution 53 (1999) 1414–1422.
[8] D.B. Carlini, R. Young, M. Vecchione, A molecular phylogeny of the Octopoda (Mollusca: Cephalopoda) evaluated in light of morphological evidence, Mol. Phylogenet. Evol. 21 (2001) 388–397.
[9] M.T. Guzik, M.D. Norman, R.H. Crozier, Molecular phylogeny of the benthic shallow-water octopuses (Cephalopoda: Octopodinae), Mol. Phylogenet. Evol. 37 (2005) 235–248.
[10] N. Kaneko, T. Kubodera, A. Iguchi, Taxonomic study of shallow-water octopuses (Cephalopoda: Octopodidae) in Japan and adjacent waters using mitochondrial genes with perspectives on octopus DNA barcoding, Malacologia 54 (2011) 97–108.
[11] J.M. Strugnell, M.D. Norman, M. Vecchione, M.T. Guzik, A.L. Allcock, The ink sac clouds octopod evolutionary history, Hydrobiologia 725 (2014) 215–235.
[12] A.L. Allcock, A. Lindgren, J.M. Strugnell, The contribution of molecular data to our understanding of cephalopod evolution and systematics: a review, J. Nat. Hist. 49 (2015) 1373–1421.
[13] R. Xu, Q. Bo, X. Zheng, A divergent lineage among *Octopus minor* (Sasaki, 1920) populations in the Northwest Pacific supported by DNA barcoding, Mar. Biol. Res. 14 (2018) 335–344.
[14] C.W. Ho, The Sequence Divergence of Mitochondrial COI Gene Indicate a Sibling Species in *Octopus marginatus* (Cephalopoda: Octopodidae) from Taiwan, Doctoral dissertation, Msc. thesis Institute of Oceanography, National Taiwan University, 2001.
[15] M.D. Norman, Cephalopods, a World Guide: Pacific Ocean, Indian Ocean, Red Sea, Atlantic Ocean, Caribbean, Arctic, Antarctic (Pp. 226), ConchBooks, Hackenheim, Germany, 2000.
[16] R. Söller, K. Warnke, U. Saint-Paul, D. Blohm, Sequence divergence of mitochondrial DNA indicates cryptic biodiversity in *Octopus vulgaris* and supports the taxonomic distinctiveness of *Octopus mimus* (Cephalopoda: Octopodidae), Mar. Biol. 136 (2000) 29–35.
[17] T.S. Leite, M. Haimovici, W. Molina, K. Warnke, Morphological and genetic description of *Octopus insularis*, a new cryptic species in the *Octopus vulgaris* complex (Cephalopoda: Octopodidae) from the tropical southwestern Atlantic, J. Molluscan Stud. 74 (2008) 63–74.
[18] A.L. Reid, N.G. Wilson, Octopuses of the Kermadec Islands: discovery and description of a new member of the Octopus 'vulgaris' complex (*O. jollyorum*, sp. nov.) and the first description of a male *Callistoctopus kermadecensis* (Berry, 1914), Bull. Auckland Museum 20 (2015) 349–368.
[19] M.D. Amor, M.D. Norman, A. Roura, T.S. Leite, I.G. Gleadall, A. Reid, C. Perales-Raya, C.C. Lu, C.J. Silvey, E.A.G. Vidal, F.G. Hochberg, X. Zheng, J.M. Strugnell, Morphological assessment of the *Octopus vulgaris* species complex evaluated in light of molecular-based phylogenetic inferences, Zool. Scr. 46 (2017) 275–288.
[20] J.L. Boore, W.M. Brown, Big trees from little genomes: mitochondrial gene order as a phylogenetic tool, Curr. Opin. Genet. Dev. 8 (1998) 668–674.
[21] C. Gissi, F. Iannelli, G. Pesole, Evolution of the mitochondrial genome of Metazoa as exemplified by comparison of congeneric species, Heredity 101 (2008) 301.
[22] J. Ren, Z. Hou, H. Wang, M. Sun, X. Liu, B. Liu, X. Guo, Intraspecific variation in mitogenomes of five crassostrea species provides insight into oyster diversification and speciation, Mar. Biotechnol. 18 (2016) 242–254.
[23] S. Sun, M. Hui, M. Wang, Z. Sha, The complete mitochondrial genome of the alvinocaridid shrimp *Shinkaicaris leurokolos* (Decapoda, Caridea): insight into the mitochondrial genetic basis of deep-sea hydrothermal vent adaptation in the shrimp, Comp. Biochem. Phys. D 25 (2018) 42–52.
[24] S.N. Song, P. Tang, S.J. Wei, X.X. Chen, Comparative and phylogenetic analysis of the mitochondrial genomes in basal hymenopterans, Sci. Rep. 6 (2016) 20972.
[25] Y. Tang, X. Zheng, H. Zhong, Q. Li, Phylogenetics and comparative analysis of the mitochondrial genomes of three violet-ringed octopuses, Zool. Scr. 48 (2019) 482–493.
[26] H. Luo, H. Li, A. Huang, Q. Ni, Y. Yao, H. Xu, B. Zeng, Y. Li, Z. Wei, G. Yu, M. Zhang, The complete mitochondrial genome of *Platysternon megacephalum peguense* and molecular phylogenetic analysis, Genes 10 (2019) 487.
[27] F. Iannelli, G. Pesole, P. Sordino, C. Gissi, Mitogenomics reveals two cryptic species in *Ciona intestinalis*, Trends Genet. 23 (2007) 419–422.
[28] Q.P. Zhao, S.H. Zhang, Z. Deng, M. Jiang, P. Nie, Conservation and variation in mitochondrial genomes of gastropods *Oncomelania hupensis* and *Tricula hortensis*, intermediate host snails of Schistosoma in China, Mol. Phylogenet. Evol. 57 (2010) 215–226.
[29] Y. Yuan, L. Kong, Q. Li, Mitogenome evidence for the existence of cryptic species in *Coelomactra antiquata*, Genes Genom. 35 (2013) 693–701.
[30] Y. Yang, Q. Li, L. Kong, H. Yu, Comparative mitogenomic analysis reveals cryptic species in *Reticunassa festiva* (Neogastropoda: Nassariidae), Gene 662 (2018) 88–96.
[31] M.N. Aydemir, E.M. Korkmaz, Comparative mitogenomics of Hymenoptera reveals evolutionary differences in structure and composition, Int. J. Biol. Macromol. 144 (2020) 460–472.
[32] R.D. Ward, T.S. Zemlak, B.H. Innes, P.R. Last, P.D. Hebert, DNA barcoding Australia's fish species, Philos. T. R. Soc. B. 360 (2005) 1847–1857.
[33] E.L. Clare, B.K. Lim, M.D. Engstrom, J.L. Eger, P.D. Hebert, DNA barcoding of Neotropical bats: species identification and discovery within Guyana, Mol. Ecol. Notes 7 (2007) 184–190.
[34] V.A. Lukhtanov, A. Sourakov, E.V. Zakharov, P.D. Hebert, DNA barcoding central Asian butterflies: increasing geographical dimension does not significantly reduce the success of species identification, Mol. Ecol. Resour. 9 (2009) 1302–1310.
[35] E.A.B. Undheim, J.A. Norman, H.H. Thoen, B.G. Fry, Genetic identification of Southern Ocean octopod samples using mt COI, CR Biol. 333 (2010) 395–404.
[36] L. Dai, X. Zheng, L. Kong, Q. Li, DNA barcoding analysis of Coleoidea (Mollusca: Cephalopoda) from Chinese waters, Mol. Ecol. Resour. 12 (2012) 437–447.
[37] A.L. Allcock, I. Barratt, M. Eléaume, K. Linse, M.D. Norman, P.J. Smith, D. Steinke, D.W. Stevens, J.M. Strugnell, Cryptic speciation and the circumpolarity debate: a case study on endemic Southern Ocean octopuses using the COI barcode of life, Deep-Sea Res. II Top. Stud. Oceanogr. 58 (2011) 242–249.
[38] B. Winnepenninckx, Extraction of high molecular weight DNA from molluscs, Trends Genet. 9 (1993) 407.
[39] O. Folmer, M. Black, W. Hoeh, R. Lutz, R. Vrijenhoek, DNA primers for amplification of mitochondrial cytochrome c oxidase subunit I from diverse metazoan invertebrates, Mol. Mar. Biol. Biotechnol. 3 (1994) 294–299.
[40] Y. Ma, Studies on the Complete Mitochondrial Genomes of *Octopus cyanea* and *Octopus conispadiceus* (Master Dissertation), Msc. thesis Fisheries College, Ocean University of China, 2015.
[41] P. McInerney, P. Adams, M.Z. Hadi, Error rate comparison during polymerase chain reaction by DNA polymerase, Mol. Biol. Int. 2014 (2014) 287430.
[42] S. Filges, E. Yamada, A. Ståhlberg, T.E. Godfrey, Impact of polymerase Fidelity on background error rates in next-generation sequencing with unique molecular identifiers/barcodes, Sci. Rep. 9 (2019) 3503.
[43] J.D. Thompson, D.G. Higgins, T.J. Gibson, Clustal w: improving the sensitivity of progressive multiple sequence alignment through sequence weighting, position-specific gap penalties and weight matrix choice, Nucleic Acids Res. 22 (1994) 4673–4680.
[44] K. Tamura, G. Stecher, D. Peterson, A. Filipski, S. Kumar, MEGA6: molecular evolutionary genetics analysis version 6.0, Mol. Biol. Evol. 30 (2013) 2725–2729.
[45] P. Librado, J. Rozas, Dnasp v5: a software for comprehensive analysis of DNA polymorphism data, Bioinformatics 25 (2009) 1451–1452.
[46] J.W. Leigh, D. Bryant, Popart: full-feature software for haplotype network construction, Methods Ecol. Evol. 6 (2015) 1110–1116.
[47] D. Posada, jModelTest: phylogenetic model averaging, Mol. Biol. Evol. 25 (2008) 1253–1256.
[48] F. Ronquist, M. Teslenko, P. van der Mark, D.L. Ayres, A. Darling, S. Höhna, B. Larget, L. Liu, M.A. Suchard, J.P. Huelsenbeck, MrBayes 3.2: efficient Bayesian phylogenetic inference and model choice across a large model space, Syst. Biol. 61 (2012) 539–542.
[49] A. Rambaut, A.J. Drummond, Tracer v1.5 [Computer Program], Retrieved from, 2007. http://beast.bio.ed.ac.uk/Tracer.
[50] L. Excoffier, H.E.L. Lischer, Arlequin suite ver 3.5: a new series of programs to perform population genetics analyses under Linux and windows, Mol. Ecol. Resour. 10 (2010) 564–567.
[51] M. Bernt, A. Donath, F. Jühling, F. Externbrink, C. Florentz, G. Fritzsch, J. Pütz, M. Middendorf, P.F. Stadler, MITOS: Improved de novo metazoan mitochondrial genome annotation, Mol. Phylogenet. Evol. 69 (2013) 313–319.
[52] D. Laslett, B. Canback, ARWEN: A program to detect tRNA genes in metazoan mitochondrial nucleotide sequences, Bioinformatics 24 (2008) 172–175.
[53] G. Benson, Tandem repeats finder: a program to analyze DNA sequences, Nucleic Acids Res. 27 (1999) 573–580.
[54] M. Zuker, Mfold web server for nucleic acid folding and hybridization prediction, Nucleic Acids Res. 31 (2003) 3406–3415.
[55] N.T. Perna, T.D. Kocher, Patterns of nucleotide composition at fourfold degenerate sites of animal mitochondrial genomes, J. Mol. Evol. 41 (1995) 353–358.
[56] J.R. Grant, P. Stothard, The CGView server: a comparative genomics tool for circular genomes, Nucleic Acids Res. 36 (2008) 181–184.
[57] D. Wang, Y. Zhang, Z. Zhang, J. Zhu, J. Yu, KaKs_Calculator 2.0: a toolkit incorporating gamma-series methods and sliding window strategies, Genom. Proteom. Bioinf. 8 (2010) 77–80.
[58] G. Vaidya, D.J. Lohman, R. Meier, SequenceMatrix: concatenation software for the

fast assembly of multi-gene datasets with character set and codon information, Cladistics 27 (2011) 171–180.
[59] S. Kalyaanamoorthy, B.Q. Minh, T.K. Wong, A. von Haeseler, L.S. Jermiin, ModelFinder: fast model selection for accurate phylogenetic estimates, Nat. Methods 14 (2017) 587.
[60] L.T. Nguyen, H.A. Schmidt, A. Von Haeseler, B.Q. Minh, IQ-TREE: a fast and effective stochastic algorithm for estimating maximum-likelihood phylogenies, Mol. Biol. Evol. 32 (2015) 268–274.
[61] R. Lanfear, P.B. Frandsen, A.M. Wright, T. Senfeld, B. Calcott, PartitionFinder 2: new methods for selecting partitioned models of evolution for molecular and morphological phylogenetic analyses, Mol. Biol. Evol. 34 (2017) 772–773.
[62] C. Saccone, C. De Giorgi, C. Gissi, G. Pesole, A. Reyes, Evolutionary genomics in Metazoa: the mitochondrial DNA as a model system, Gene 238 (1999) 195–209.
[63] Z.A. Doubleday, J.M. Semmens, A.J. Smolenski, P.W. Shaw, Microsatellite DNA markers and morphometrics reveal a complex population structure in a mer-obenthic octopus species (*Octopus maorum*) in south-East Australia and New Zealand, Mar. Biol. 156 (2009) 1183–1192.
[64] A.A. Moreira, A.R.G. Tomas, A.W.S. Hilsdorf, Evidence for genetic differentiation of *Octopus vulgaris* (Mollusca, Cephalopoda) fishery populations from the southern coast of Brazil as revealed by microsatellites, J. Exp. Mar. Biol. Ecol. 407 (2011) 34–40.
[65] X. Gao, X. Zheng, Q. Bo, Q. Li, Population genetics of the common long-armed octopus *Octopus minor* (Sasaki, 1920) (Cephalopoda: Octopoda) in Chinese waters based on microsatellite analysis, Biochem. Syst. Ecol. 66 (2016) 129–136.
[66] M. Nei, W.H. Li, Mathematical model for studying genetic variation in terms of restriction endonucleases, P. Natl. Acad. Sci. 76 (1979) 5269–5273.
[67] A. Eimanifar, R.T. Kimball, E.L. Braun, J.D. Ellis, Mitochondrial genome diversity and population structure of two western honey bee subspecies in the Republic of South Africa, Sci. Rep. 8 (2018) 1–11.
[68] S.I. Yokobori, N. Fukuda, M. Nakamura, T. Aoyama, T. Oshima, Long-term conservation of six duplicated structural genes in cephalopod mitochondrial genomes, Mol. Biol. Evol. 21 (2004) 2034–2046.
[69] T. Akasaki, M. Nikaido, K. Tsuchiya, S. Segawa, M. Hasegawa, N. Okada, Extensive mitochondrial gene arrangements in coleoid Cephalopoda and their phylogenetic implications, Mol. Phylogenet. Evol. 38 (2006) 648–658.
[70] R. Cheng, X. Zheng, X. Lin, J. Yang, Q. Li, Determination of the complete mitochondrial DNA sequence of *Octopus minor*, Mol. Biol. Rep. 39 (2012) 3461–3470.
[71] R. Cheng, X. Zheng, Y. Ma, Q. Li, The complete mitochondrial genomes of two octopods *Cistopus chinensis* and *Cistopus taiwanicus*: revealing the phylogenetic position of the genus *Cistopus* within the order Octopoda, PLoS One 8 (2013) e84216.
[72] X. Zhang, X. Zheng, Y. Ma, Q. Li, Complete mitochondrial genome and phylogenetic relationship analyses of *Amphioctopus aegina* (Gray, 1849) (Cephalopoda: Octopodidae), Mitochondrial DNA 28 (2015) 17–18.
[73] J.F. Domínguez-Contreras, A. Munguia-Vega, B.P. Ceballos-Vázquez, F.J. García-Rodriguez, M. Arellano-Martinez, The complete mitochondrial genome of *Octopus bimaculatus* Verrill, 1883 from the Gulf of California, Mitochondrial DNA 27 (2016) 4584–4585.
[74] S. Sun, Q. Li, L. Kong, H. Yu, Multiple reversals of strand asymmetry in molluscs mitochondrial genomes, and consequences for phylogenetic inferences, Mol. Phylogenet. Evol. 118 (2018) 222–231.
[75] E.P.C. Rocha, M. Touchon, E.J. Feil, Similar compositional biases are caused by very different mutational effects, Genome Res. 16 (2006) 1537.
[76] X.Q. Cai, G.H. Liu, H.Q. Song, C.Y. Wu, F.C. Zou, H.K. Yan, Z.G. Yuan, R.Q. Lin, X.Q. Zhu, Sequences and gene organization of the mitochondrial genomes of the liver flukes *Opisthorchis viverrini* and *Clonorchis sinensis* (Trematoda), Parasitol. Res. 110 (2012) 235–243.
[77] G.H. Liu, S.Y. Wang, W.Y. Huang, G.H. Zhao, S.J. Wei, H.Q. Song, M.J. Xu, R.Q. Lin, D.H. Zhou, X.Q. Zhu, The complete mitochondrial genome of *Galba pervia* (Gastropoda: Mollusca), an intermediate host snail of *Fasciola* spp, PLoS One 7 (2012) e42172.
[78] X. Zheng, Y. Ma, R. Cheng, Application of mitochondrial DNA in phylogenetic analysis of Cephalopods, J. Fish. China 39 (2015) 294–303 (in Chinese).
[79] J.M. Strugnell, N.E. Hall, M. Vecchione, D. Fuchs, A.L. Allcock, Whole mitochondrial genome of the Ram's Horn Squid shines light on the phylogenetic position of the monotypic order Spirulida (Haeckel, 1896), Mol. Phylogenet. Evol. 109 (2017) 296–301.
[80] G.S. Wilkinson, A.M. Chapman, Length and sequence variation in evening bat D-loop mtDNA, Genetics 128 (1991) 607–617.
[81] D.J. Stanton, L.L. Daehler, C.C. Moritz, W.M. Brown, Sequences with the potential to form stem-and-loop structures are associated with coding-region duplications in animal mitochondrial DNA, Genetics 137 (1994) 233–241.
[82] J.E. Faber, C.A. Stepien, Tandemly repeated sequences in the mitochondrial DNA control region and phylogeography of the pike-perchesstizostedion, Mol. Phylogenet. Evol. 10 (1998) 310–322.
[83] F. Ye, S.D. King, D.K. Cone, P. You, The mitochondrial genome of Paragyrodactylus variegatus (Platyhelminthes: Monogenea): differences in major non-coding region and gene order compared to Gyrodactylus, Parasit. Vectors 7 (2014) 377.
[84] D.T. Amaral, Y. Mitani, Y. Ohmiya, V.R. Viviani, Organization and comparative analysis of the mitochondrial genomes of bioluminescent Elateroidea (Coleoptera: Polyphaga), Gene 586 (2016) 254–262.
[85] O. Tomoko, Synonymous and nonsynonymous substitutions in mammalian genes and the nearly neutral theory, J. Mol. Evol. 40 (1995) 56–63.
[86] S. Sun, Q. Li, L. Kong, H. Yu, Complete mitochondrial genomes of *Trisidos kiyoni* and *Potiarca pilula*: varied mitochondrial genome size and highly rearranged gene order in Arcidae, Sci. Rep. 6 (2016) 33794.
[87] E.M. Perkins, S.C. Donnellan, T. Bertozzi, I.D. Whittington, Closing the mitochondrial circle on paraphyly of the Monogenea (Platyhelminthes) infers evolution in the diet of parasitic flatworms, Int. J. Parasitol. 40 (2010) 1237–1245.
[88] J.A. Baeza, F.A. Sepúlveda, M.T. González, The complete mitochondrial genome and description of a new cryptic species of *Benedenia Diesing*, 1858 (Monogenea: Capsalidae), a major pathogen infecting the yellowtail kingfish *Seriola lalandi* Valenciennes in the South-East Pacific, Parasite Vector 12 (2019) 490.
[89] M.W. Jacobsen, R.R. da Fonseca, L. Bernatchez, M.M. Hansen, Comparative analysis of complete mitochondrial genomes suggests that relaxed purifying selection is driving high nonsynonymous evolutionary rate of the NADH2 gene in whitefish (*Coregonus* ssp.), Mol. Phylogenet. Evol. 95 (2016) 161–170.
[90] M.S. Acosta-Jofré, R. Sahade, J. Laudien, M.B. Chiappero, A contribution to the understanding of phylogenetic relationships among species of the genus *Octopus* (Octopodidae: Cephalopoda), Sci. Mar. 76 (2011) 311–318.
[91] J.E. Uribe, R. Zardoya, Revisiting the phylogeny of Cephalopoda using complete mitochondrial genomes, J. Molluscan Stud. 83 (2017) 133–144.
[92] S. Khatami, P. Tavakoli-Kolour, T. Valinassab, F.E. Anderson, A. Farhadi, Molecular identification and phylogenetic relationships of Coleoidea (Mollusca: Cephalopoda) from the Persian Gulf and Oman Sea reveals a case of cryptic diversity, Mollus. Res. 38 (2018) 77–85.
[93] D.B. Carlini, L.K. Kunkle, M. Vecchione, A molecular systematic evaluation of the squid genus *Illex* (Cephalopoda: Ommastrephidae) in the North Atlantic Ocean and Mediterranean Sea, Mol. Phylogenet. Evol. 41 (2006) 496–502.
[94] S.B. Johnson, A. Warén, R.C. Vrijenhoek, DNA barcoding of *Lepetodrilus* limpets reveals cryptic species, J. Shellfish Res. 27 (2008) 43–51.
[95] F.L. Mantelatto, P.R. Pezzuto, A. Masello, C.L.D.B.R. Wongtschowski, A.W.S. Hilsdorf, N. Rossi, Molecular analysis of the commercial deep-sea crabs *Chaceon ramosae* and *Chaceon notialis* (Brachyura, Geryonidae) reveals possible cryptic species in the South Atlantic, Deep-Sea Res. Pt. I. 84 (2014) 29–37.
[96] K.R. Andrews, A.J. Williams, I. Fernandez-Silva, S.J. Newman, J.M. Copus, C.B. Wakefield, J.E. Randall, B.W. Bowen, Phylogeny of Deepwater snappers (Genus *Etelis*) reveals a cryptic species pair in the indo-Pacific and Pleistocene invasion of the Atlantic, Mol. Phylogenet. Evol. 100 (2016) 361–371.
[97] K. De Queiroz, Species concepts and species delimitation, Syst. Biol. 56 (2007) 879–886.